



Cite this: DOI: 10.1039/d5fb00934k

# Chitosan/PVA/gelatin derived biodegradable coatings enriched with *Rosa rubiginosa* for extended shelf life and preservation of strawberries

Beenish Sarwar,<sup>a</sup> Muhammad Zubair,<sup>b</sup> Asma Yaqoob,<sup>c</sup> Faiz Ahmed,<sup>d</sup> Sohail Shahzad<sup>\*a</sup> and Aman Ullah<sup>id</sup><sup>\*b</sup>

This study developed biodegradable composite coatings and films using chitosan (CS), polyvinyl alcohol (PVA), and gelatin enriched with *Rosa rubiginosa* extract (RRE) to enhance the shelf life of strawberries. The coatings were prepared through solution blending and applied *via* dip-coating, while the corresponding films were fabricated using solution casting. FTIR and SEM analyses confirmed the effective molecular interactions and uniform microstructure within the composite matrix. Increasing the proportion of RRE improved functional performance by reducing the moisture content, water solubility, water absorption, and oxygen permeability. The formulation with the highest RRE content (BS-03) exhibited the strongest antioxidant activity ( $78.8 \pm 1.01\%$  DPPH inhibition;  $IC_{50} = 0.3 \text{ mg mL}^{-1}$ ) and enhanced antibacterial potential against *Staphylococcus aureus*, *Bacillus subtilis*, and *Escherichia coli*. Soil burial tests revealed that the films were biodegradable, with BS-02 and BS-03 showing mass losses of up to 91.29% and 86.79% after 45 days, respectively. When applied to strawberries, the coatings significantly reduced weight loss and delayed visible spoilage, extending the shelf life by up to 10 days compared to uncoated fruit. Sensory evaluation also confirmed better color, firmness, and acceptability of the coated samples. These findings demonstrate that CS/PVA/gelatin coatings enriched with RRE offer a promising, safe, and eco-friendly approach for prolonging the freshness of perishable fruits.

Received 9th December 2025  
Accepted 31st January 2026

DOI: 10.1039/d5fb00934k

rsc.li/susfoodtech

## Sustainability spotlight

Biodegradable coatings developed from chitosan, polyvinyl alcohol, gelatin, and *Rosa rubiginosa* extract present an environmentally friendly technique for fruit preservation. These natural and synthetic biopolymers are combined to produce films with improved antioxidant, antibacterial and barrier properties, providing a sustainable alternative to traditional plastic packaging. By applying these coatings to strawberries, the study shows a significant increase in the shelf life while minimizing food waste and environmental impact. The addition of *Rosa rubiginosa*, a plant rich in bioactive compounds, enhances the value of underutilized botanical resources. This work aligns with the goals of circular bioeconomy and supports the global transition to sustainable, biodegradable materials for food packaging applications.

## 1. Introduction

Approximately 1.3 billion tons of food is wasted annually, making food waste one of the major global challenges of our time, which results in resource depletion and environmental damage.<sup>1</sup> Packaging protects food from harmful ultraviolet rays and preserves its quality, aroma, taste, and physicochemical

characteristics. By preserving food, we can enhance its use and protect it from microbial decay.<sup>2</sup> With the increasing demand for eco-friendly packaging solutions, innovative biopolymer-based coatings play a vital role in preserving food and prolonging the shelf life of perishable items, thereby positively affecting the environment.<sup>3</sup> Films containing plasticizers such as glycerol, honey, and propylene glycol are applied to food products to improve their nutritional, antimicrobial, and antioxidant properties.<sup>4</sup> The addition of natural extracts, such as essential oils or plant extracts, to chitosan-based films improves their functional properties.<sup>5</sup> A variety of semi-synthetic and edible biopolymers are used in food packaging applications, including chitosan, agarose, alginate, agar, starch, cellulose, guar gum, polyvinyl alcohol and carboxymethyl cellulose.<sup>6,7</sup> Although plastic materials are lightweight, economical, and flexible, they contribute to waste, raising environmental concerns.<sup>3</sup>

<sup>a</sup>Department of Chemistry, University of Sahiwal, Sahiwal 57000, Pakistan. E-mail: drsohail@uosahiwal.edu.pk

<sup>b</sup>Lipid Chemistry Utilization Lab, Department of Agricultural, Food & Nutritional Science, University of Alberta, Edmonton, AB, T6G 2P5, Canada. E-mail: ullah2@ualberta.ca

<sup>c</sup>Institute of Biochemistry, Biotechnology and Bioinformatics, The Islamia University of Bahawalpur, Pakistan

<sup>d</sup>Department of Chemistry, Government College University Faisalabad, Faisalabad 37000, Pakistan



Recently, there has been growing interest in utilizing biodegradable materials for food packaging and coatings.<sup>8</sup> Bio-based plastics are favoured for film coatings because they are abundantly available, biodegradable and capable of forming films.<sup>9</sup> However, these materials often lack mechanical strength and offer poor resistance.<sup>10</sup> To address these limitations, structural modifications<sup>11</sup> or blending of bio-based polymers with synthetic polymers have been performed to obtain specific properties.<sup>12</sup> Chitosan, a naturally occurring biopolymer with inherent anti-microbial<sup>13</sup> and anti-oxidant properties,<sup>14–16</sup> has been widely used in food packaging.<sup>17</sup> It is non-toxic<sup>18</sup> and has chelating ability to bind with vital trace metals selectively and bacteria, and to prevent toxin and bacterial growth,<sup>19,20</sup> thus making it suitable for food packaging applications.<sup>21,22</sup> In addition, chitosan has high susceptibility to water and low thermal and mechanical strength, which limits its use in food packaging materials. To address these limitations, different techniques such as cross-linking,<sup>23–26</sup> enzymatic treatment,<sup>27</sup> graft copolymerization,<sup>28–30</sup> complex formation,<sup>29</sup> surface coating,<sup>31</sup> incorporation of fillers,<sup>32</sup> high-energy radiation<sup>33</sup> and blending with other biopolymers or synthetic polymers can be used.<sup>34,35</sup>

PVA is a synthetic and water-soluble polymer that is an ideal biomaterial for making polymer blends. It is biocompatible, flexible, and non-toxic<sup>36</sup> and can be used in food packaging applications because of its low cost, eco-friendly nature, durability, transparency, mechanical strength, chemical stability, and film-forming properties.<sup>37,38</sup> Blending PVA with chitosan not only enhanced the mechanical strength but also improved the antibacterial activity of the fabricated films.

In contrast, *Rosa rugosa*, a common petal variety, has been traditionally used in biomedical applications.<sup>39</sup> *Rosa* species contain components including flavonoids, terpenes, glycosides, polyphenols, and anthocyanins. The volatile oil extracted from *Rosa* flowers possesses therapeutic properties and is primarily used for analgesic, anticonvulsant, cardiovascular, and laxative purposes.<sup>40</sup> Given the numerous bioactive components found in *Rosa rubiginosa* (RR), our objective was to explore the effects of its incorporation and proportion when combined with CS/PVA/gelatin solutions. These coatings and films are expected to exhibit enhanced mechanical strength and improved antibacterial, antioxidant, and biodegradable properties, which are essential for prolonging the shelf life of coated or packaged food products, such as strawberries. Choi *et al.* developed a ternary blend (CS/PVA/gelatin)-based composite film incorporating *Duchesnea indica* extract for the preservation of strawberries.<sup>41</sup> In another study, Islam *et al.* fabricated packaging films using a casting methodology with CS/PVA incorporated with zinc oxide nanoparticles and dragon fruit waste extract. The incorporation of ZnO nanoparticles and dragon fruit waste extract enhanced the thermal and mechanical strength and provided antioxidant and antibacterial potential to the films.<sup>42</sup> Similarly, Wang *et al.* synthesized bilayered films with excellent biodegradable, antibacterial, mechanical, and oxygen barrier properties using CS as the outer layer and PVA/gelatin as the inner layer loaded with 2.5% curcumin nanoparticles for the preservation of fish (bigeye tuna).<sup>43</sup> However, CS/PVA/gelatin ternary

films have not yet been combined with RRE, and their application as edible coatings for strawberries has not been evaluated in terms of antioxidant/antibacterial performance, barrier properties, biodegradability, and sensory acceptance. This study aims to develop and characterize CS/PVA/gelatin coatings enriched with varying concentrations of RRE and evaluate their effectiveness in extending the shelf life of strawberries.

## 2. Experimental

### 2.1 Materials

The chemicals and solvents utilized in this study were employed directly as obtained from manufacturers or redistilled when necessary. Macklin Chemicals (China) supplied chitosan (CS) with a deacetylation degree exceeding 95% (molecular weight ( $M_w$ ) 100–200 kDa) and viscosity in the range of 100–200 mPa s. Polyvinyl alcohol (PVA) ( $M_w$  72 000 with 98% degree of hydrolysis) was procured from Merck (Germany). Gelatin and glacial acetic acid ( $C_2H_4O_2$ ) were bought from Sigma Aldrich–Germany. A taxonomist identified the plant sample as *Rosa rubiginosa* (RR), which was obtained from the University of Sahiwal, Pakistan. Strawberries were purchased from a local market in Sahiwal–Pakistan.

### 2.2 Methodology

**2.2.1 Preparation of *Rosa rubiginosa* extract (RRE).** The flower petals of *Rosa rubiginosa* were thoroughly washed with deionized water to remove any debris or impurities present on the surface, followed by air drying at room temperature (20–25 °C) for 10–12 days. The petals were ground to make a powder, and then a 5% w/v aqueous solution of *Rosa rubiginosa* was prepared by refluxing at 60 °C with a centrifugal force of 125.8g for 4 hours. The solution was filtered with Whatman filter paper number 1, under vacuum conditions, and the filtrate was stored at 4 °C for further use to fabricate coatings and films (Fig. S3).

**2.2.2 Preparation of CS/PVA/gelatin derived coatings and films loaded with RRE.** The CS/PVA/gelatin based composite coatings and the final films were produced by blending individual component solutions and then using a conventional solution casting methodology, as described by Rubilar *et al.*<sup>44</sup> A 1% chitosan (w/v) solution was prepared by dissolving 1 g of chitosan in a 1% acetic acid solution, with stirring at room temperature for a duration of 72 hours. Similarly, a 5% PVA (w/v) solution was prepared by dissolving 5 g of PVA in the respective amount of deionized water by refluxing at 80 °C for 5 hours. A 2% (w/v) Gelatin solution was made by dissolving 2 g of gelatin in deionized water. A 30% (v/v) glycerol solution was made by combining 30 mL glycerol with the required amount of deionized water. Then, different volume proportions of CS, PVA, gelatin, glycerol, and RRE (Table 1) were combined and stirred for 48 hours at room temperature to form a uniform solution. The resulting solutions were then used for dip coating of strawberries and were also used for evaluation of the antioxidant and antibacterial potential. The other part of the solution was cast in Petri dishes and kept at room temperature, to fabricate composite films, for characterization and evaluation



Table 1 Different volume ratios of all solutions for coatings and film formation

Samples codes	CS solution (mL)	PVA solution (mL)	Glycerol solution (mL)	Gelatin solution (mL)	RRE (mL)
BS-0	20	20	10	2	0
BS-01	20	20	10	2	2
BS-02	20	20	10	2	4
BS-03	20	20	10	2	6

of certain other properties. The solution was evaporated within 2 to 3 days and films were formed, after which they were removed from the dishes (Fig. 1).

### 2.3 Characterization of the synthesized films

**2.3.1 FTIR analysis.** All composite fabricated films were characterized by using a FTIR spectrometer (Thermo Nicolet 6700P, Waltham, Massachusetts, USA), to evaluate interactions among individual components and to identify peaks of prominent functional groups of the films. Spectra were acquired in photo acoustic mode, with a range of  $4000\text{--}400\text{ cm}^{-1}$ , using carbon background and helium purging with  $8\text{ cm}^{-1}$  resolution and 256 scans.

**2.3.2 Thickness of the fabricated films.** The thickness of the fabricated films in millimetres (mm) was noted by using a digital thickness gauge (manufactured by Insize company, China), with 0–10 mm range, 0.01 mm resolution and  $\pm 0.02$  mm accuracy. Reported thickness values are the mean values of

five random values taken at various positions, including the edges and centre.

**2.3.3 Camera images.** Camera images of the synthesized films were taken to evaluate the appearance, homogeneity, colour and texture. Images were taken using the camera of an Infinix Hot-30 play made by Infinix Mobile China, Dual-LED flash, HDR, panorama (16 MP, f/1.8, wide, PDAF, QVGA, 1080p@30fps).

**2.3.4 Scanning electron microscopy (SEM) analysis.** To investigate the surface and cross-sectional microstructure of the fabricated films, SEM analysis was conducted using the EmCrafts Cube II tabletop model from South Korea. The samples were sputter-coated and placed on SEM holders, with images captured at different magnifications using an accelerating voltage of 10 kV.

**2.3.5 Dynamic mechanical analysis (DMA).** Mechanical properties of the films were evaluated by measuring the tensile strength and elongation at break using a dynamic mechanical analyzer (DMA) Q800 manufactured by TA Instruments (USA)

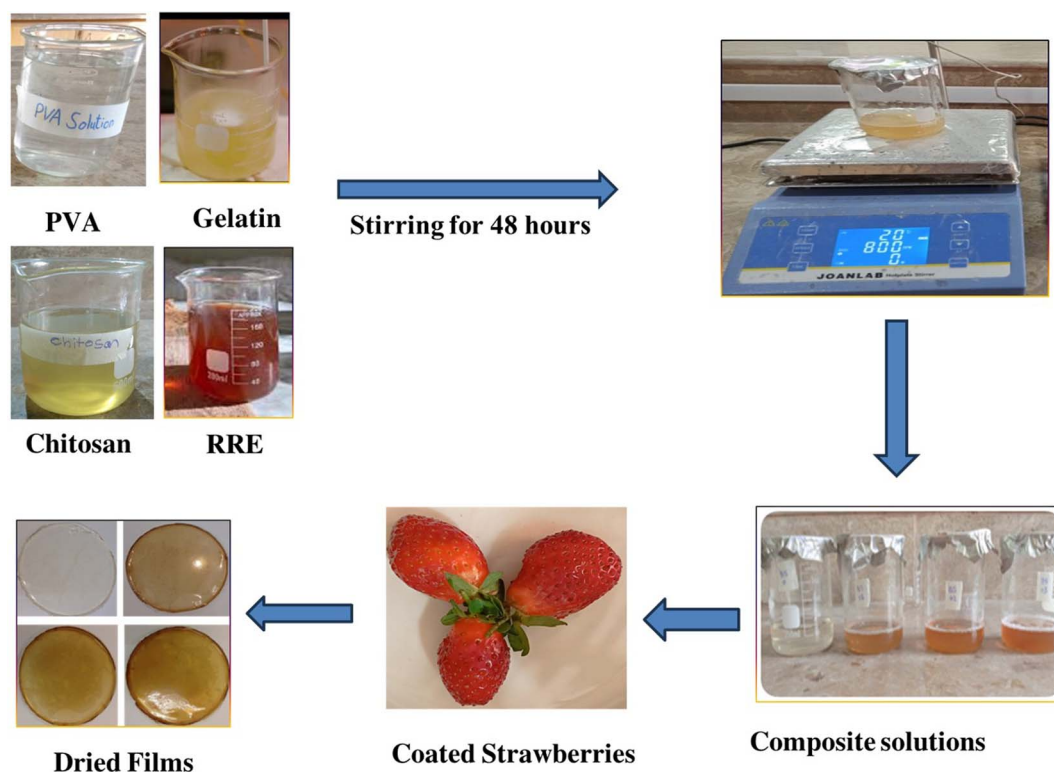


Fig. 1 Preparation of composite CS/PVA/gelatin coatings and films loaded with RRE.



with software version of V21.3 Build 96 using a controlled force module. The films were cut into  $6 \times 3$  cm size and analysed by the method equilibrated at  $50^\circ\text{C}$ , isothermal for 5 minutes and ramp force 3 newton per minute to 18 newton per minute.

**2.3.6 X-ray diffraction (XRD) analysis.** XRD analysis was performed to analyse the crystalline/amorphous nature of fabricated CS/PVA/gelatin enriched with RRE films using an XRD powder system, D8 advance, model cube 10, EmCrafts manufactured by Bruker, South Korea. Film spectra were recorded in the range of  $10\text{--}70^\circ$  with 20 seconds per step and 0.09 step size.

**2.3.7 Percent moisture content (MC %) determination.** The percentage moisture content was determined using the loss on drying method. Initially, small sections of the film samples were cut, and their weight was measured. These samples were then placed in an oven set at  $80^\circ\text{C}$  for one hour and weighed again with precision. This process was repeated until the weight remained constant. The moisture content percentage (MC %) was calculated using eqn (1).<sup>45,46</sup>

$$\text{MC}(\%) = \frac{M_w - M_d}{M_w} \times 100 \quad (1)$$

where  $M_w$  stands for the initial weight of the film samples before drying, conditioned at 53% relative humidity to moisture equilibrium, and  $M_d$  stands for the dried weight. The average moisture content percentage was determined from three replications.

**2.3.8 Water solubility percent (WS %).** Small pieces of the films were cut and placed in an oven at  $80^\circ\text{C}$  for 1 hour and then their dried weight was measured. The films were then introduced into Petri dishes containing 25 mL of distilled water for 24 hours to maximize their solubility in water. The films were then removed from the Petri dishes and were dried in an oven at  $80^\circ\text{C}$  until they attained a constant weight. The water solubility percent (WS %) was evaluated from the following formula:<sup>47</sup>

$$\text{WS } \% = \frac{W_i - W_f}{W_i} \times 100 \quad (2)$$

where  $W_i$  stands for the initially dried weight in grams and  $W_f$  stands for the final/terminal dried weight (g). For each measurement, three readings were taken and then WS % was evaluated by taking the mean reading.

**2.3.9 Water absorption pattern of the films.** Small pieces of the films were cut and their dried weight was measured. These pieces were put into Petri dishes containing 10 mL distilled water, so that the films can absorb maximum water and can swell by retaining water within their structure. The water absorption behavior of each film was observed by keeping the films dipped in water for 10 minutes followed by their removal and subsequent weight measurement. After weighing, the films were again immersed in water, and the process was repeated until they achieved constant weight. The percentage water absorption capacity of each film was determined by using the following formula:<sup>48</sup>

$$\text{Water absorption}(\%) = \frac{W_s - W_d}{W_d} \times 100$$

where  $W_s$  stands for the swollen weight and  $W_d$  stands for the dried weight.

**2.3.10 Water drop test.** A piece of the film was placed over a support raised from a table and a water drop was poured onto the film surface. Then a pass or fail judgment was given depending on whether the drop passed through the film or not.<sup>49,50</sup>

**2.3.11 Oxygen permeability.** Winkler's method, which measures dissolved oxygen in  $\text{mg mL}^{-1}$ , was employed to assess the oxygen permeability of CS/PVA/gelatin/RRE films.<sup>51</sup> In this process, distilled water was placed in glass bottles sealed with the composite films using a sealant, and the quantity of oxygen that permeated through them was measured.

**2.3.12 Antibacterial potential of CS/PVA/gelatin/RRE coating solutions.** The antibacterial potential of the CS/PVA/gelatin coating solution and RRE-infused CS/PVA/gelatin solutions was evaluated against two Gram-positive bacterial strains, *S. aureus* and *B. subtilis*, as well as one Gram-negative strain, *E. coli*. This assessment was conducted using the standard method previously described.<sup>52</sup> A suspension of 100  $\mu\text{L}$  for each of the two bacterial strains, containing approximately  $10^7$  colony-forming units (CFUs) per mL, was prepared. The bacterial cells were cultured in nutrient broth (Oxoid, UK) for around 8 hours at  $37^\circ\text{C}$ . Using a sterilized swab, the bacterial culture was evenly distributed on agar plates, which were then allowed to dry for 15 minutes. Filter discs soaked with CS/PVA/gelatin/RRE solutions were placed on the agar plates, with four discs, each containing a different sample, positioned equidistantly on each test plate. A separate Petri dish, containing a filter disc impregnated with the commercially available antibiotic ciprofloxacin at a concentration of  $10 \mu\text{g mL}^{-1}$  served as a positive control. Before incubating the plates at  $37^\circ\text{C}$  for 17–24 hours, they were refrigerated at  $4^\circ\text{C}$  for two hours. The inhibition zones produced by each sample were measured in millimetres using a pair of calipers, indicating the antibacterial potential of each sample and the positive control. The experiments were conducted in triplicate to ensure reliability.

**2.3.13 Antioxidant potential of CS/PVA/gelatin/RRE coating solutions.** The antioxidant properties of samples containing CS/PVA/gelatin infused with RRE were assessed using the 2,2-diphenylpicrylhydrazyl (DPPH) method. This technique, commonly employed to evaluate the antioxidant potential of samples with plant extracts, is highly regarded for its stability, practicality, and reliability. The level of antioxidant activity is gauged by the components' ability, particularly plant-based ones like flavonoids and polyphenolics, to neutralize the DPPH radical. In this method, a sample was prepared by mixing 20  $\mu\text{L}$  of solution with 3 mL of distilled water. Then, 1 mL of this mixture was added to 0.2 mL of a methanolic DPPH solution (1 mM). The resulting mixture was kept in the dark at room temperature for about 40 minutes. The absorbance of the solution was measured at 517 nm against a blank using a UV-visible spectrophotometer. This procedure was conducted three times, and the percentage of DPPH radical scavenging activity was calculated using a specific formula:<sup>45,46</sup>



$$\text{Scavenging activity (SA \%)} = \frac{A_{\text{control}} - A_{\text{sample}}}{A_{\text{control}}} \times 100$$

where  $A_{\text{control}}$  shows the absorbance of the control, that is DPPH solution, and  $A_{\text{sample}}$  stands for the absorbance of the samples.

**2.3.14 Biodegradation test.** Film samples were cut into small strips for evaluation of their biodegradation behavior. The experiment utilized 200 g of dry soil collected from the Sahiwal field area, which was then moistened by spraying distilled water. Four polythene cups were filled with equal amounts of this prepared soil. The film samples were buried at a consistent depth within the soil and maintained at room temperature with 70% relative humidity. After 15 days, the condition of the films was evaluated based on their visual appearance and weight loss. Subsequently, the samples were reburied in the soil and examined again after 45 days to assess their further degradation.<sup>48</sup>

**2.3.15 Total flavonoid contents (TFCs).** TFCs of RRE with a concentration of 5 mg mL<sup>-1</sup> were assessed by a procedure already described in the literature with a few modifications.<sup>53</sup> This is the same concentration which was incorporated into CS/PVA/gelatin films. For this assay, freshly prepared reagents including 1 M NaOH, 5% NaNO<sub>2</sub> and 10% Al<sub>2</sub>Cl<sub>3</sub> were used. The assay involved taking 1 mL of RRE in a test tube and then adding 400  $\mu$ L of NaNO<sub>2</sub> and 6 mL of distilled water. The mixture was thoroughly blended to ensure maximum homogeneity. The mixture was incubated for 10 minutes, followed by addition of 700  $\mu$ L of Al<sub>2</sub>Cl<sub>3</sub> (10%) and 3 mL of NaOH (1 M). The absorbance was subsequently recorded at 510 nm using an STA-8100ST UV/Vis spectrophotometer from Van Nuys, Los Angeles, CA, USA, to assess TFCs as catechin equivalents per unit of dry matter.

**2.3.16 Total phenolic contents (TPCs).** The Folin-Ciocalteu method was employed to determine the TPCs of RRE.<sup>53</sup> RRE solution was prepared at a concentration of 5 mg mL<sup>-1</sup>. Then 200  $\mu$ L of RRE was taken into test tubes and 1000  $\mu$ L of the Folin-Ciocalteu reagent was added, followed by vigorous blending and mixing of solutions. Subsequently, 800  $\mu$ L of Na<sub>2</sub>CO<sub>3</sub> (7.5%) was introduced into the solution, which was then left at room temperature for 2 hours. The mixture was thoroughly combined, and the absorbance of the resulting solution was recorded at 765 nm using an STA-8100ST UV/Vis spectrophotometer (Van Nuys, Los Angeles, CA, USA). Gallic acid served as the standard for quantifying the TPCs, which were expressed as GAE (Gallic Acid Equivalents) per gram of dry weight of powdered samples (GAE per g). Each sample was analysed in triplicate.

**2.3.17 Application of composite coatings on strawberries.** The potential of the synthesized solutions was evaluated as a coating application on strawberries to increase their shelf life using the dip coating technique.<sup>54</sup> The synthesized composite solutions of CS/PVA/gelatin incorporating RRE possess antibacterial and antioxidant potential, which was believed to provide better protection of strawberries against their early decomposition. The various solutions used for coatings on strawberries were coded as BS-0, BS-01, BS-02 and BS-03, with the only difference being increase in RRE from 0 mL in BS-0 to 2

mL into BS-01, 4 mL into BS-02 and finally 6 mL into BS-03. Thus, it was believed that increasing the RRE volume ratio from 0 mL (BS-0) to 6 mL in BS-03 would also enhance its potential to protect strawberries. Initially, fresh and healthy strawberries were obtained, which were cleaned with tissue paper to eliminate dirt, and then thoroughly dried. The prepared solutions were then applied to the dried strawberries using the dip-coating method. Each strawberry's weight was recorded, and they were then stored at room temperature for 17 days with 50% relative humidity. The decay and deterioration of the strawberries, along with their weight loss, were regularly monitored. Thus, the study examined the extension of shelf life and preservation of their freshness. Strawberry samples were tested in triplicate, with their weight loss percent recorded for each. The average value was then used for calculations.

$$\text{Weight loss(\%)} = \frac{W_i - W_f}{W_i} \times 100$$

where  $W_i$  stands for the initial weight of strawberries and  $W_f$  stands for the final weight of strawberries.

**2.3.18 Sensory evaluation.** The sensory assessment of coated strawberries was performed according to Nowacka *et al.* (2018)<sup>55</sup> for all formulations, including BS-0, BS-01, BS-02 and BS-03 and a control without any coating. The parameters such as taste, smell, color, juiciness, firmness and acceptance in general were noted on a scale of 0 to 10. A score of 8 was seen as exceptional, additional desired, juicy and acceptable whereas a score of 1 was regarded as poor, extra unwanted, dry and unsuitable.

**2.3.19 Statistical analysis.** Statistical analysis of data was performed through analysis of variance (two-way-ANOVA) using the software Origin Pro 2022, Origin Lab Corporation, Northampton, Massachusetts (USA). All measurements from the tests were taken in triplicate ( $n = 3$ ), and the data results are presented as the mean  $\pm$  standard deviation (SD). The error bars on column graphs in all figures represent the standard deviation among three replicates, which is a measure of data variability and reproducibility. Differences between means were evaluated by Tukey's multiple range test ( $p < 0.05$ ).

## 3. Results and discussion

### 3.1 FTIR analysis

FTIR analyses were performed to determine the various functional groups present in the films synthesized from CS/PVA/gelatin and loaded with RRE and to check their intermolecular interactions. Fig. 2 shows the FTIR spectra of CS/PVA/gelatin films without RRE (BS-0) and with RRE (BS-01, BS-02 and BS-03). FTIR spectra of all films in Fig. 2 show a very broad peak at 3300 cm<sup>-1</sup> to 3250 cm<sup>-1</sup> due to the overlapping stretching frequencies of hydroxyl O-H and amino N-H groups.<sup>46</sup> Alkyl C-H group asymmetric stretching was observed between 2950 cm<sup>-1</sup> and 2916 cm<sup>-1</sup>. The peaks for the amide I and amide II bands appeared at 1669 cm<sup>-1</sup> and 1564 cm<sup>-1</sup>, respectively.<sup>56</sup> CH<sub>2</sub> bending peaks were seen at 1408 cm<sup>-1</sup> and 1338 cm<sup>-1</sup>. C-O and C-O-C stretching vibrations were observed at 1143 cm<sup>-1</sup> and 1099 cm<sup>-1</sup>. These vibration bands were also reported by Dawei



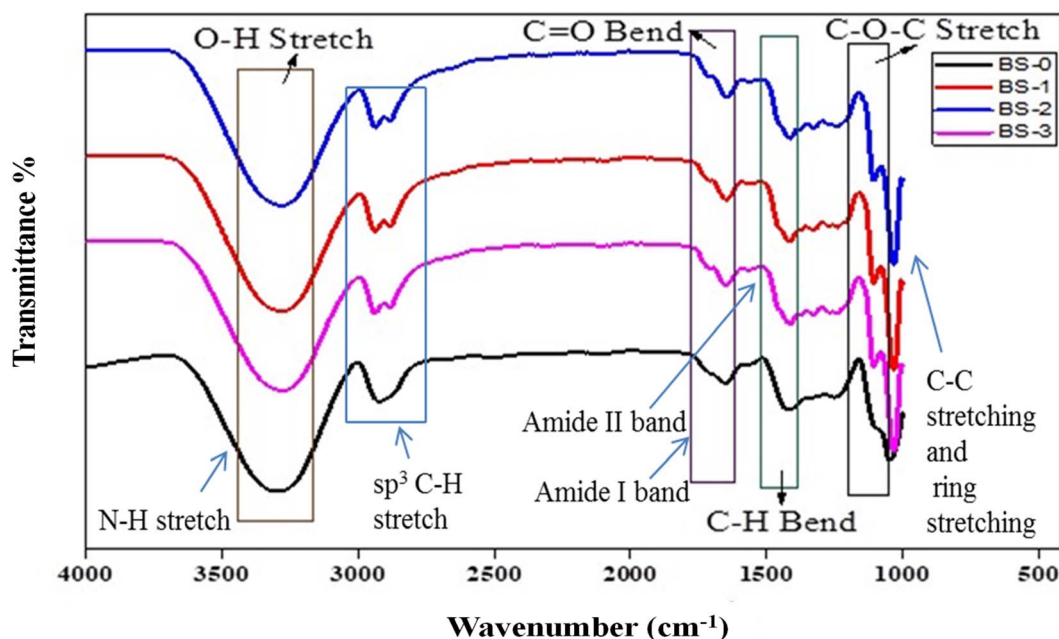


Fig. 2 FTIR spectra of BS-0, BS-01, BS-02 and BS-03 films.

Yun *et al.*<sup>57</sup> Chitosan's ring stretching vibrations appeared in the fingerprint region at  $895\text{ cm}^{-1}$ .<sup>58</sup>

The FTIR spectra of the films with RRE exhibited an additional prominent peak at  $2970\text{ cm}^{-1}$  attributed to aromatic C-H stretch,<sup>59</sup> which was due to aromatic polyphenolic and flavonoid compounds present in RRE. Similarly, FTIR spectra of BS-01, BS-02 and BS-03 exhibited numerous small peaks from  $1800\text{ cm}^{-1}$  to  $1500\text{ cm}^{-1}$ , due to additional components of RRE.<sup>60</sup> Minor variations towards lower frequency for certain peaks were observed in the FTIR spectra, possibly due to bonding interactions between CS, PVA, gelatin and RRE. Additional peaks at  $1700\text{ cm}^{-1}$ , present in BS-01, BS-02 and BS-03 spectra and absent in the BS-0 spectrum, were attributed to various components like secondary metabolites and polyphenols present in RRE.<sup>61</sup> The BS-0 film displayed O-H and N-H stretching at  $3330\text{ cm}^{-1}$ , and the band shifted towards lower wavenumber at  $3267\text{ cm}^{-1}$  for films incorporated with RRE (BS-01, BS-02 and BS-03), due to the greater interactions, created by active functional groups O-H and N-H present within CS, PVA, gelatin and RRE. As the OH group present in polyphenols develops hydrogen bonding with the OH group present in CS and PVA, and  $\text{NH}_2$  group in chitosan, greater hydrogen bonding results in lower frequency ranges. These FTIR results are also supported by literature studies.<sup>62</sup> The hydroxyl group ( $-\text{OH}$ ) and amino group ( $-\text{NH}_2$ ) stretching vibrations in the BS-0 film spectrum appeared to be greater than those found in BS-01, BS-02, and BS-03 spectra. This was due to the presence of a higher number of unreacted  $-\text{OH}$  and  $-\text{NH}_2$  functional groups in the BS-0 film. The reduction in stretching vibrations in the spectra of BS-01, BS-02, and BS-03 films containing RRE suggested the involvement of active  $-\text{OH}$  and  $-\text{NH}_2$  groups in PVA and chitosan with the functional groups present in RRE, leading to the formation of hydrogen bonds and other weak electrostatic

interactions. Overall, FTIR analysis confirmed the presence of the characteristic peaks for all components under consideration.

### 3.2 Film thickness

The thickness of the films is a vital factor in attaining desirable optical properties and optimum barrier against water and vapor transfer. An increase in film thickness may reduce the diffusion rates of oxygen and water vapors of the film.<sup>63</sup> The addition of plasticizers, antioxidants, and antimicrobial agents can increase the thickness of the films, offering better barrier properties and improved mechanical strength.<sup>64</sup> The thickness results shown in Fig. 3 indicate that the BS-0 film (without RRE) showed a minimum thickness of  $0.123 \pm 0.02\text{ mm}$ , while the maximum thickness was displayed by BS-03 ( $0.884 \pm 0.06\text{ mm}$ ), followed by BS-02 ( $0.771 \pm 0.05\text{ mm}$ ), and BS-01 ( $0.439 \pm 0.03\text{ mm}$ ). Gradually increasing the RRE from 0 mL (BS-0) to 6 mL (BS-03) also enhanced the film thickness, which is consistent with the literature.<sup>65</sup> Films with suitable or greater thicknesses offer better barrier properties, and thus lower water and oxygen permeability, making them ideal for prolonged packaging of perishable fruits.

### 3.3 Visual impact by camera images

The visual appearance and color of films are essential parameters that affect the standard and quality of food items. Colored films have more potential to wrap food items and preserve them because they reduce oxidation reactions in packaged foods.<sup>66</sup> Fig. 4 shows the camera images of the CS/PVA/gelatin films and CS/PVA/gelatin films loaded with various volumes of RRE. The CS/PVA/gelatin films were completely transparent, whereas the other films incorporating RRE were yellowish-brown. It was noted that, by increasing the RRE volume from 2 mL in BS-01 to



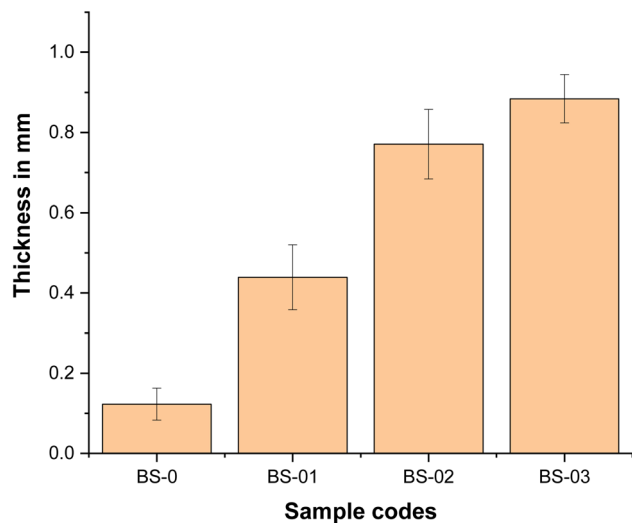


Fig. 3 Film thicknesses of the composite films.

6 mL in BS-03, the color of the films became intense yellowish brown as illustrated in Fig. 4. Additionally, the films were seen smooth due to better mixing, blending and developing certain types of new interactions between film components. The dried films were observed to be smooth, homogeneous, stretchable, bubble free, mechanically strong, and flexible and they were peeled off from the Petri dishes swiftly without cracks.

### 3.4 Morphological analysis using SEM

SEM analysis was used to examine the surface morphology of the prepared CS/PVA/gelatin film and CS/PVA/gelatin loaded with RRE films. The SEM images of the composite films are shown Fig. 5. The SEM images in Fig. 5(a–c) of the BS-0 film (composed of only CS/PVA/gelatin) appear clearer and more homogenous without cracks and crystalline particles/aggregates on their surface, indicating the amorphous nature of this film. The micrographs in Fig. 5(d–f) of the BS-01 film show that all components were uniformly distributed and appeared in one phase and were homogeneous. The images show the presence of certain aggregates/crystals within the structure, which were due to the addition of 2 mL of RRE into the CS/PVA/gelatin matrix. The addition of RRE into the CS/PVA/gelatin matrix has induced certain intermolecular interactions, thus producing a few aggregates of some components. The micrographs in

Fig. 5(g–i) represent the BS-02 film incorporating CS/PVA/gelatin loaded with 4 mL of RRE. Here also, the images reveal the uniformity, consistency and homogeneity of all the added components. Additionally, the BS-02 film also showed many white crystals, which might have been formed due to the interactions between active functional groups in CS, PVA, gelatin and RRE. Thus, it is evident from the images that increasing the RRE ratio from 2 mL (BS-01) to 4 mL (BS-02) had altered the morphology of the films to some extent. The film with a higher volume ratio of RRE (4 mL in BS-02) exhibited more crystalline molecules/aggregates within its structure, as already reported in the literature.<sup>67</sup> One potential explanation is the interaction between the active components of RRE and the active groups in CS, PVA, and gelatin, which leads to the partial release of bioactive compounds such as polyphenols, alkaloids, and amino acids onto the film's surface.<sup>68</sup> A similar type of interaction was also reported by Han *et al.* in Noni (*Morinda citrifolia*) fruit polysaccharide enriched with blueberry leaf extract.<sup>69</sup> It is believed that bridging phenomena occurred inside the bio-composite films in which some molecules of RRE bonded to the CS chain while the rest of the functional groups attached to another CS chain. Thus, the overall surface morphology shows that RRE was effectively incorporated into the CS/PVA/gelatin solution matrix. In contrast to the above results, Fig. 5(j–l) represents the BS-03 film (incorporating 6 mL of RRE), which shows the film structure as clearer, smoother and more homogeneous, without a higher number of crystalline particles/aggregates on its surface as compared to the BS-02 film. Thus, it can be concluded that increasing the RRE to 6 mL in the CS/PVA/gelatin matrix would again make the film texture smooth.<sup>70</sup>

The cross-sectional analysis of the BS-0 film is shown in Fig. 6(a), which shows that the film is homogeneous, uniform, thick, and has no cracks in its structure. Similarly, the cross-sectional SEM image of the BS-01 film is more homogeneous, uniform and without any pores as compared to the BS-02 film, which has certain cracks in its structure.

Further cross-sectional images in Fig. 6(c and d) reveal that BS-02 and BS-03 films incorporating RRE addition to CS/PVA and gelatin were smoother, and their thickness increased, respectively. The increase in thickness was primarily due to the increasing volume ratios of RRE. The BS-02 film cross-sectional image in Fig. 6(c) shows some cracks and irregular cavities, which indicates its changed morphology as compared to other

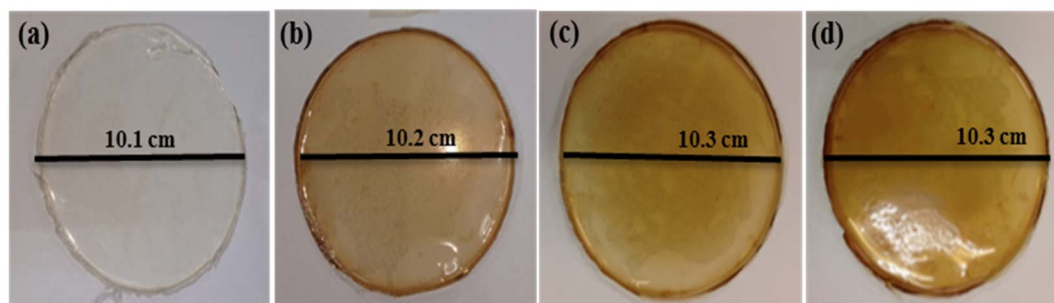


Fig. 4 Visual appearances of the composite films: (a) BS-0, (b) BS-01, (c) BS-02, and (d) BS-03.



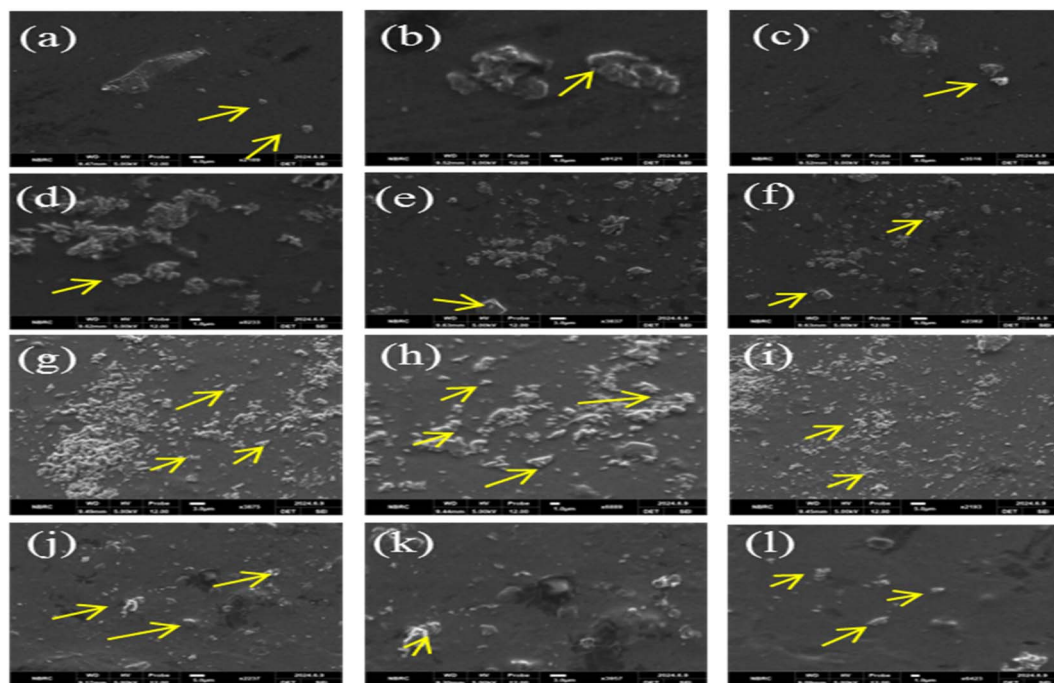


Fig. 5 SEM micrographs of BS-0 (a–c), BS-01 (d–f), BS-02 (g–i) and BS-03 (j–l) films.

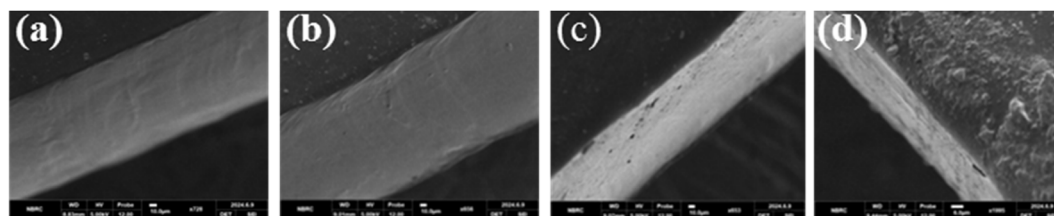


Fig. 6 Cross-sectional film images: BS-0 (a), BS-01 (b), BS-02 (c) and BS-03 (d).

films. This indicated the presence of certain types of intermolecular interactions between functional groups of RRE active constituents and CS, PVA and gelatin.

The BS-03 film also appeared smooth and without cracks/pores. The homogeneous distribution of bioactive components within the matrix of the films ensures that their antibacterial and antioxidant activities remain unaffected.

### 3.5 Mechanical strength

The mechanical properties of films are crucial for their use in packaging. To assess the mechanical strengths of these films, stress–strain curves were plotted and are depicted in Fig. 7. Two sample films, including BS-0 (incorporating CS/PVA/gelatine) and BS-03 (incorporating CS/PVA/gelatine and RRE) were selected for the determination of mechanical properties and to evaluate the effect of incorporation of RRE into the CS/PVA/gelatin matrix. The BS-0 film stress–strain curve is shown in green colour, while the BS-03 stress–strain curve is shown in red colour. It was noted that the addition of RRE had slightly reduced the mechanical properties of the films. The stress value for the BS-0 film was noted as 0.32 MPa, while the stress value

for the BS-03 film was 0.21 MPa. Similarly, the strain % for the BS-01 film was noted as 56%, while for the BS-03 film it was nearly 25%. This phenomenon can be explained as follows: RRE contains many polyphenolic and flavonoid components, which have active functional groups. These active functional groups had created certain interactions with polymeric chains of CS, PVA and gelatin. Thus, polymeric interactions among CS, PVA and gelatin chains were reduced, which ultimately altered the internal structure of the films. It is well known that chitosan has low mechanical strength; thus, it is blended with synthetic polymers like PVA to enhance its mechanical strength. The introduction of aqueous RRE into the CS/PVA/gelatin film (BS-03) has reduced its deformation, made the film stiffer and more rigid, and less flexible. Young's modulus for the BS-0 film was calculated to be 0.57 MPa, while Young's modulus for the BS-03 film was calculated to be 0.86 MPa. Thus the BS-03 film was observed to be less deforming, stiffer and more rigid as compared to the BS-01 film. Thus the BS-03 film is suitable for applications which require more strength and dimensional stability such as packaging applications. However the BS-01 film was deformed more under higher stress, which exhibits its



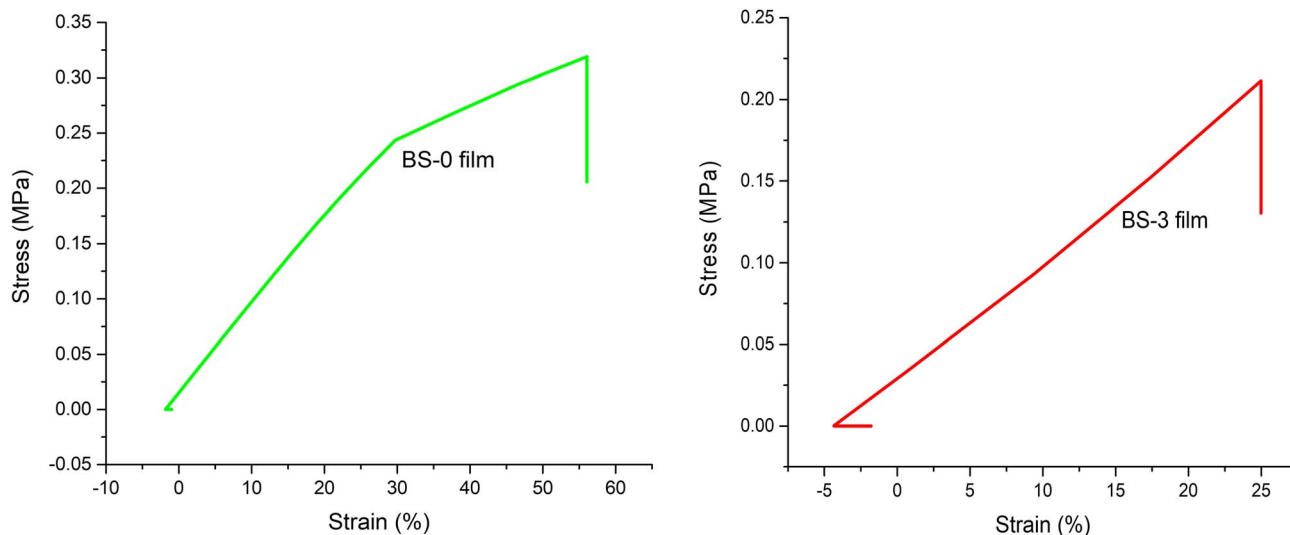


Fig. 7 Mechanical properties of CS/PVA/gelatin and CS/PVA/gelatin/RRE films.

higher flexibility and better suitability for those applications where flexibility and stretchability are required.

### 3.6 XRD analysis

XRD analysis was performed to determine the crystalline or amorphous nature of the composite films. Literature studies of PVA and CS XRD spectra showed that PVA had a prominent peak at  $2\theta = 39.9^\circ$ , while CS exhibited a sharp peak at  $2\theta = 20^\circ$ . The BS-0 coded film demonstrated two notable peaks, one at  $2\theta = 19.59^\circ$  corresponding to the crystalline phase of chitosan, and another at  $2\theta = 39.9^\circ$  representing the amorphous phase as a lower intensity shoulder. The CS/PVA film BS-01 containing RRE also showed two amorphous peaks, slightly shifted to  $2\theta = 20^\circ$  and  $2\theta = 41.9^\circ$ . The BS-02 film exhibited peaks at  $19.9^\circ$  and  $39.6^\circ$ , while the BS-03 film displayed intensified peaks at  $20.2^\circ$

and  $42^\circ$ . Additional peaks were observed in BS-01, BS-02, and BS-03 films due to the inclusion of RRE, as illustrated in Fig. 8. The XRD values obtained for CS/PVA/gelatin films and CS/PVA/gelatin loaded with RRE films were found to be aligned with previously reported values.<sup>71</sup> These XRD results confirmed the various interactions between CS, PVA, gelatin and RRE within the film matrix.

### 3.7 Moisture content percent of the films

The moisture content of polymer-based films is a crucial parameter to determine the quality of films, as the purpose of films is to preserve the food from microbial spoilage. Here, CS/PVA/gelatin and CS/PVA/gelatin enriched with RRE composite films were analyzed for their ability to absorb moisture, and the results are displayed in Fig. 9(A), and the values are mentioned

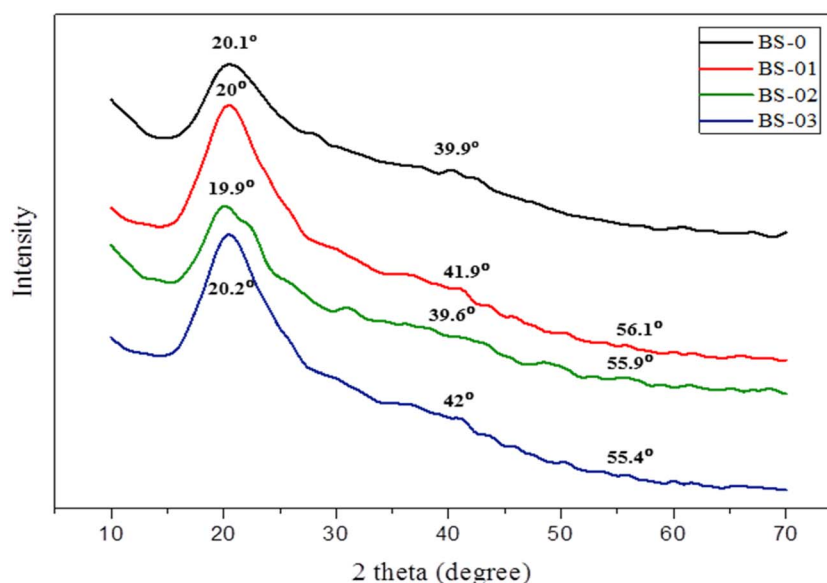


Fig. 8 XRD patterns of the composite films.



in Table 2. The outcomes of this assay revealed that all the films absorbed moisture content from 15% to 17%. Thus, a small variation was observed in moisture content results, which could be attributed to their different compositions. The moisture absorption phenomenon could be explained based on interactions such as hydrogen bonds between active amino and hydroxyl groups of CS, hydroxyl groups of PVA and water. In addition to this, the presence of glycerol had also contributed to moisture absorption, as glycerol is a well-known humectant. Furthermore, it was noted that the incorporation of RRE into the CS/PVA/gelatin matrix had slightly lessened the percent moisture content of the films. As the ratio of RRE was increased in the CS/PVA/gelatin matrix, the moisture content percent was decreased to a small extent. The reported results are in accordance with literature studies, as it has been mentioned in the literature that CS and PVA produced more interactions with active components of RRE and ultimately, their interaction with water was decreased, which led to hydrophobicity and a slight reduction of moisture content.<sup>72</sup> The decreased percent moisture content is most favourable for food packaging applications as it offers better water barrier properties by lowering the microbial growth and improving the texture of packaged food.<sup>71</sup>

### 3.8 Percent water solubility

The percent solubility of composite films of CS/PVA/gelatin and CS/PVA/gelatin loaded with RRE in water is the measure of weight loss of films when fully immersed in water for 24 hours. Solubility percent determination is important to measure as it depicts the stability of films as and when they come in contact with moisture in the environment for a longer time. The

solubility percent test results are presented in Fig. 9(B), and their exact values are also given in Table 2. It was noticed that the CS/PVA/gelatin film BS-0 shows a maximum solubility % of 73%, which is mainly due to the presence of hydrophilic polymers of PVA and gelatin. However, CS is hydrophobic, and it makes interactions with both PVA and gelatin within the films to decrease their solubility. The addition of RRE into CS/PVA/gelatin films had decreased their solubility, as the BS-01 film solubility was 70.2%. Furthermore, increasing the volume ratio of RRE in the CS/PVA/gelatin films further decreased the solubility of the films, as observed in BS-02 (63.2% solubility) and BS-03 films (60.2% solubility). The intense interaction between CS and other polymers such as PVA, gelatin, and RRE led to increased intermolecular bonding, which in turn reduced their solubility.<sup>73</sup> The films with lower solubility rates are more beneficial for food packaging applications, as these films are more likely to compromise with the moisture present in the surroundings, and their dissolution rate slows down. However, a balance between solubility and biodegradability is important, as excessively low solubility may slow down the degradation process post-use. A similar phenomenon of reducing the solubility of films by incorporating tea extract was also reported by Hafsa *et al.*<sup>74</sup>

### 3.9 Water absorption

Water absorption percent of films is a vital indicator to check their quality to absorb and retain water within their structure without being dissolved or solubilized. The degree of water absorption was found to be inversely proportional to the degree of interactions or crosslinking among different constituents of

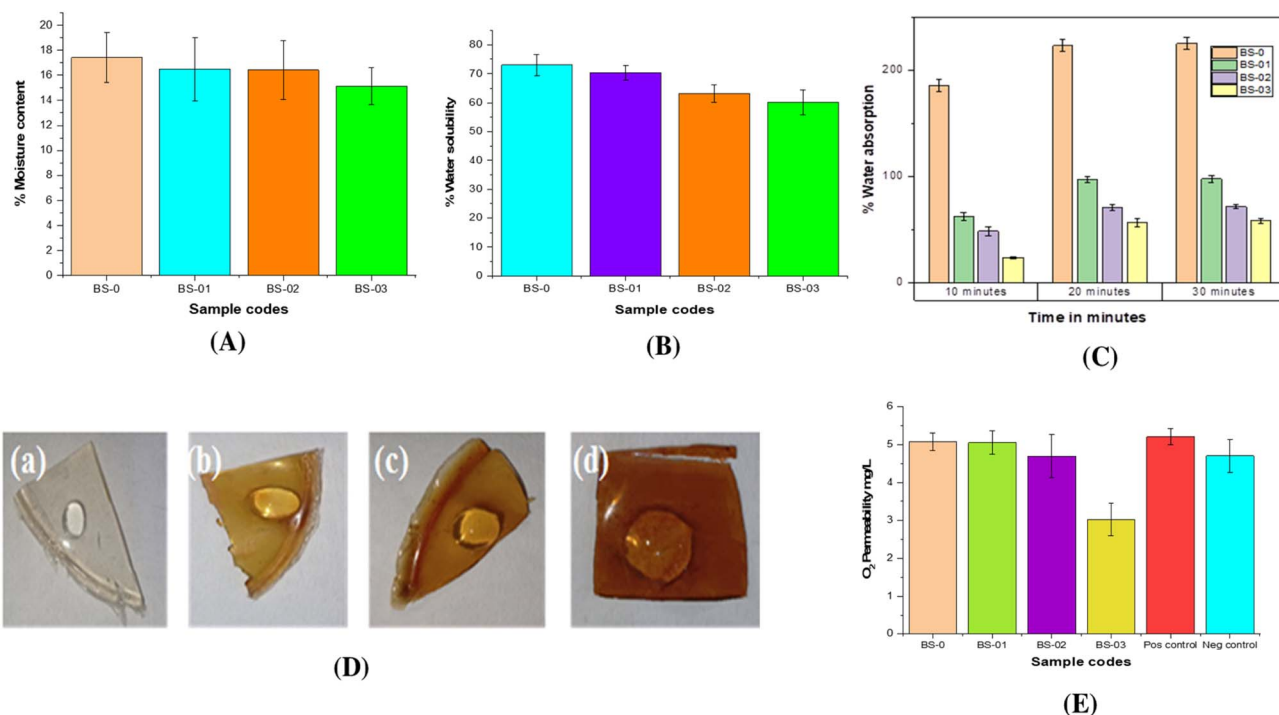


Fig. 9 (A) % Moisture content, (B) % water solubility, (C) % water absorption, and (D) water drop test on films (a) BS-0, (b) BS-01, (c) BS-02 and (d) BS-03. (E) Oxygen permeability results of the prepared films.



Table 2 Film thickness, % moisture content, % solubility and % water absorption values (mean  $\pm$  standard deviation)

S. no.	Sample codes	Film thickness (mm)	Moisture content (%)	Water solubility (%)	Water absorption (%)
1	BS-0	0.123 $\pm$ 0.04	17.42 $\pm$ 1.97	73 $\pm$ 3.6	225.3 $\pm$ 5.25
2	BS-01	0.439 $\pm$ 0.081	16.51 $\pm$ 2.52	70.2 $\pm$ 2.52	97.7 $\pm$ 3.44
3	BS-02	0.771 $\pm$ 0.087	16.41 $\pm$ 2.35	63.2 $\pm$ 3.07	71.4 $\pm$ 1.97
4	BS-03	0.884 $\pm$ 0.06	15.14 $\pm$ 1.46	60.2 $\pm$ 4.35	58.23 $\pm$ 2.31

films. More interactions or crosslinking between polymeric chains show lesser water absorption and *vice versa*. The films with lower water absorption percent are frequently opted for food packaging applications. The results of the water absorption percent test are shown in Fig. 9(C) and listed in Table 2. The results exhibited that the BS-0 film absorbed maximum water up to 225.3% for 30 minutes. The BS-01, BS-02 and BS-03 films showed 97.7%, 71.4% and 58.23% of water absorption, respectively. The higher absorption by the BS-0 film can be attributed to the presence of hydrophilic polymers such as PVA and gelatin, which, in the absence of RRE, had made more interactions with water and thus absorbed more. The other films showed less absorption due to the presence of RRE and more interactions/crosslinking of polymeric chains with RRE instead of water molecules. This is evident because as the RRE volume ratio is enhanced, % water absorption is decreased, due to apparent development of a higher degree of crosslinking which resulted in lower % water absorption.<sup>75</sup>

### 3.10 Water drop test

A water drop test was performed on the composite films to check their ability to allow water to pass through or not. The films that hold water appeared to be acceptable for their application in food packaging. The test results for all films are displayed in Fig. 9(D), and the results show that the films did not allow the water drop to pass through them. The films or other materials which show superior water barrier properties are often opted for in food packaging applications.<sup>76</sup>

### 3.11 Oxygen permeability

Oxygen permeability of films has a noteworthy effect on the quality and shelf life of packaged food items. When oxygen enters the films, it causes spoilage of food items by oxidation, microbial growth and colour changes. Thus, lower rates of oxygen permeability can inhibit the oxidative spoilage and growth of aerobic microbes, leading to extended shelf life of perishable food products like strawberries. The oxygen present in the atmosphere can also weaken the bond energy of polymers, and thus unstable peroxides are formed. These unstable species slow down the degradation rate of polymeric films and thus make them unsuitable for food packaging applications. The oxygen permeability of the composite films was evaluated by the method already discussed by Wrinkler, and the results are presented in Fig. 9(E).<sup>77</sup>

The O<sub>2</sub>-permeability test results for an airtight flask (negative control) and an open flask (positive control) were 4.7  $\pm$  0.43 mg L<sup>-1</sup> and 5.21  $\pm$  0.22 mg L<sup>-1</sup>, respectively. The oxygen

permeability values calculated for each film were 5.08  $\pm$  0.23 mg per L (BS-0), 5.05  $\pm$  0.31 mg per L (BS-01), 4.69  $\pm$  0.57 mg per L (BS-02) and 3.03  $\pm$  0.43 mg per L (BS-03). The data demonstrated that incorporating RRE reduced oxygen permeability, due to increasing RRE volume, which caused free volumetric holes in the films to contract, making it more difficult for oxygen molecules to penetrate. Thus, lower oxygen permeability is a desirable characteristic for polymers, particularly in food packaging applications.<sup>78</sup>

### 3.12 Antibacterial potential

Natural plant extracts incorporating antibacterial components are more sterile, eco-friendly, and biodegradable. They are regarded as excellent materials to be used in food packaging against food pathogens.<sup>79</sup> Plant extracts contain bioactive phenolic and flavonoid components, and the hydroxyl groups in these compounds provide the basis for their antibacterial activity. The hydroxyl groups develop certain interactions, such as hydrogen bonds, with the bacterial cell membrane. Based on their hydrophobic nature, these phenolic compounds may accumulate on the surface of cells or may invade the cytoplasm of microbes. After reaching the cytoplasm, these components interact with the other cellular organelles and cell's components; thus, they change the pH inside the cell membrane.<sup>80</sup> The bacterial cell wall has negative carboxylate groups (-COO<sup>-</sup>) and chitosan carries positive amino groups (-NH<sub>3</sub><sup>+</sup>). The electrostatic interactions of these groups with each other provide the mechanism for antibacterial activity.<sup>81</sup> CS/PVA/gelatine and CS/PVA/gelatine incorporating RRE solutions were assessed for antibacterial potential against *S. aureus*, *B. subtilis* and *E. coli*, and the results are shown in Fig. 10(A and B) and Table 3. The effectiveness of each coating solution was determined by measuring the inhibition zone in mm. All the coating solutions exhibited fair to good antibacterial potential against all three bacterial strains in comparison to the control. The results demonstrated that in most tests, the BS-03 sample showed better results than other samples. This was due to the presence of a higher volume ratio of RRE in the BS-03 sample. When we compared the results of all samples, BS-03 showed higher % inhibition against *S. aureus* with the lowest IC<sub>50</sub> value of 78.65  $\pm$  0.13. Similarly, the BS-02 sample exhibited higher activity against *E. coli* with the lowest IC<sub>50</sub> value of 118.6  $\pm$  0.021; while the BS-03 sample exhibited the highest potential against *B. subtilis* with the lowest IC<sub>50</sub> value of 128.75  $\pm$  0.65. Overall, BS-02 and BS-03 samples incorporating higher volume ratios of RRE showed better antibacterial potential against all three bacterial strains as compared to BS-0 and BS-01, attributed to the presence of various active components (phenolic compounds, flavonoids, and others) in the RRE. Notably, the increasing volume of RRE correlated with improved antibacterial activity.



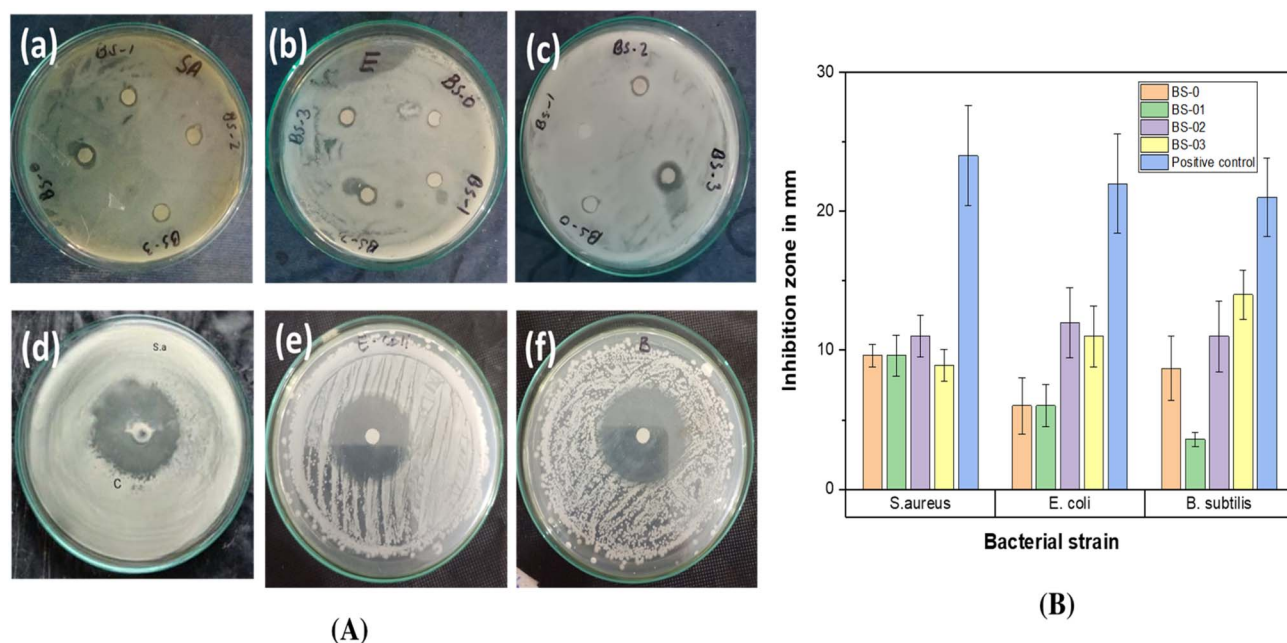


Fig. 10 (A) Anti-bacterial images of samples against (a) *S. aureus* (b) *E. coli* (c) *B. subtilis*, and (d–f) representing positive controls for *S. aureus*, *E. coli* and *B. subtilis*, respectively; (B) anti-bacterial potential of samples in terms of the inhibition zone in mm.

Based on these findings, the synthesized CS/PVA/gelatine/RRE films, especially BS-02 and BS-03, show promise for food packaging applications. Similar antibacterial results were also reported by Dan *et al.*<sup>82</sup> for a chitosan–gelatin film incorporating hop plant extract. The natural compounds found in plants are considered ideal candidates for food packaging applications due to their antibacterial properties. Two-way ANOVA demonstrated that the treatment type significantly influenced antibacterial activity ( $p < 0.001$ ), and its effect varied among bacterial species. The positive control produced the strongest

inhibition zones, BS-02 and BS-03 had moderate effects, while BS-0 and BS-01 showed minimal inhibition. These results suggest that specific treatments possess promising antibacterial potential depending on the bacterial species tested.

### 3.13 Antioxidant potential

The enhancement in food shelf life and its preservation applications depend upon the antioxidant potential of the synthesized coating solutions and films. Oxidation reactions cause discoloration of food and reduce its flavor. Antioxidant

Table 3 Antibacterial properties of all synthesized sample solutions

Sample code	Inhibition zone (mm)	IC <sub>50</sub> at 100 mg mL <sup>-1</sup>	Percent inhibition
<b><i>S. aureus</i></b>			
BS-0	9.6	172.91 ± 0.0542	17.12 ± 0.0542
BS-01	9.6	122.91 ± 0.047	31 ± 0.047
BS-02	11	93.6 ± 0.049	38.57 ± 0.049
BS-03	8.9	78.65 ± 0.13	38.57 ± 0.13
Control	24	50 ± 0.9	100.714
<b><i>E. coli</i></b>			
BS-0	6	120 ± 0.014	40 ± 0.014
BS-01	6	115 ± 0.09	40 ± 0.09
BS-02	12	118.6 ± 0.021	33.6 ± 0.021
BS-03	11	120 ± 0.028	23 ± 0.028
Control	22	50 ± 0.8	100
<b><i>B. subtilis</i></b>			
BS-0	8.7	138 ± 0.604	40 ± 0.234
BS-01	3.6	225 ± 0.234	39.47368421
BS-02	11	189.64 ± 0.28	26.10526316 ± 0.28571
BS-03	14	128.75 ± 0.65	37.89473684 ± 0.65
Control	21	50.85 ± 0.714	100.714



materials are required to deactivate and scavenge free radicals. The antioxidant potential of solutions was determined by the 2,2-diphenyl-1-picrylhydrazyl (DPPH) assay (Table 4). DPPH is a nitrogen-free stable radical of deep purple color, which turns yellow after reacting with antioxidants. Antioxidant capacity was determined using the  $IC_{50}$  values, which represent the sample mass per mL of DPPH required to reduce the DPPH concentration by 50%. The results in Fig. 11 indicate that the BS-03 film demonstrated superior antioxidant properties ( $78.8 \pm 1.01$  with  $IC_{50}$  value of  $0.3 \text{ mg mL}^{-1}$ ) attributed to the presence of plant extract (RRE) in excess. Similarly, the BS-02 sample showed an antioxidant potential of  $70.5 \pm 0.57$  with an  $IC_{50}$  value of  $0.5 \text{ mg mL}^{-1}$ . The BS-01 film exhibited an antioxidant potential of  $58.23 \pm 1.3$  with an  $IC_{50}$  value of  $0.7 \text{ mg mL}^{-1}$ . The lowest antioxidant activity was exhibited by the BS-0 sample having an antioxidant potential value of  $47.0 \pm 0.51$  with an  $IC_{50}$  value of  $1.1 \text{ mg mL}^{-1}$ . The enhanced antioxidant activities of BS-03, BS-02 and BS-01 as compared to BS-0 were clearly attributed to the numerous active components found in RRE, including flavonoids, phenolics, citronellol, nerol, quercetin, catechin, epicatechin, rutin and phenethyl alcohol. These compounds prevent oxidative degradation, thus preventing the food from microbial spoilage and resulting in prolonging freshness. The results were also in accordance with the literature analysis.<sup>83</sup> A statistical analysis reveals that both concentration and treatment type have highly significant effects on antioxidant activity. Furthermore, there is a significant interaction between these factors, indicating that the effect of each treatment depends on the concentration used. Thus, higher concentration significantly increases antioxidant activity ( $p < 0.0001$ ).

### 3.14 Biodegradation of the composite films

A soil burial degradation test was conducted to evaluate the decomposition rate of the prepared films. The weight loss percentage with respect to the number of days for BS-0, BS-01, BS-02, and BS-03 films was measured. This method effectively indicated film biodegradability due to the presence of microbes and moisture in soil. The biodegradation process is initiated with water absorption, which disrupts hydrogen bonding between polymeric chains, followed by microbial invasion from bacteria, algae, and fungi. Biodegradation is a natural process and is also influenced by the chemical composition of composite films. Various factors affect polymeric film degradation rates, including pollutant quantity, microbial presence, and environmental

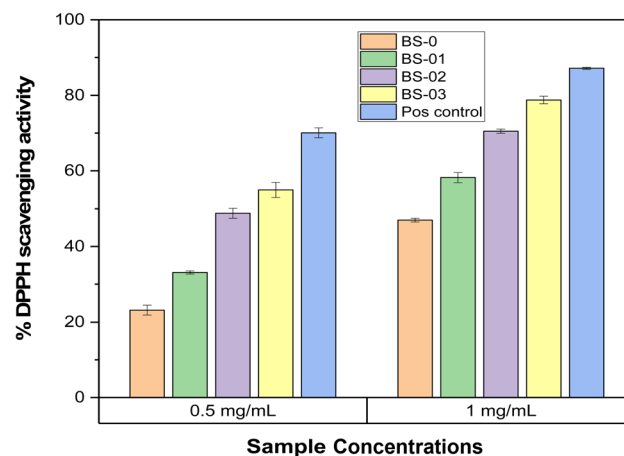


Fig. 11 Antioxidant potential of the sample films and positive control.

conditions (oxygen, humidity, pH, and temperature). Fig. 12(A) displays the degraded film images after 18 and 45 days, while Fig. 12(B) shows the % biodegradation after 18 and 45 days. The results showed that the BS-02 film demonstrated the highest % degradation of 91.29%, followed by the BS-03 film at 86.79% and the BS-01 film at 85.91%, while the BS-0 film showed a % degradation of 81.48%. It was observed that incorporation of RRE into CS/PVA/gelatin has improved the % biodegradation of the films. The biodegradation rates were higher as compared to already reported results by Riaz *et al.*<sup>84</sup> The increased % biodegradation, due to the incorporation of RRE, was attributed to the presence of carbon, nitrogen, and oxygen in many components of RRE, which served as food sources for microorganisms. Continuous water addition activates soil bacteria and weakens polymeric interactions between components, thus increasing degradation rates.<sup>85</sup> The incorporation of RRE into CS/PVA/gelatin films improved their biodegradability, transforming them into a rapidly degradable and eco-friendly material.<sup>84</sup> The faster degradation of these biopolymer films in soil environments provides a sustainable alternative with reduced environmental impact.

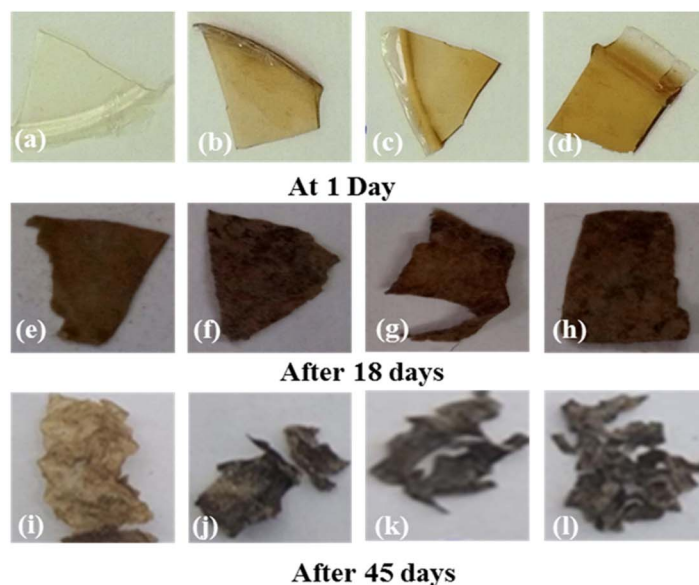
### 3.15 Total phenolic contents (TPCs) and total flavonoid contents (TFCs)

Polyphenols constitute the most frequent and broadly distributed group of compounds in the plant kingdom, with more than 8000 currently known compounds.<sup>86</sup> The rose flower has high polyphenolic compounds and essential oil, and thus serves as

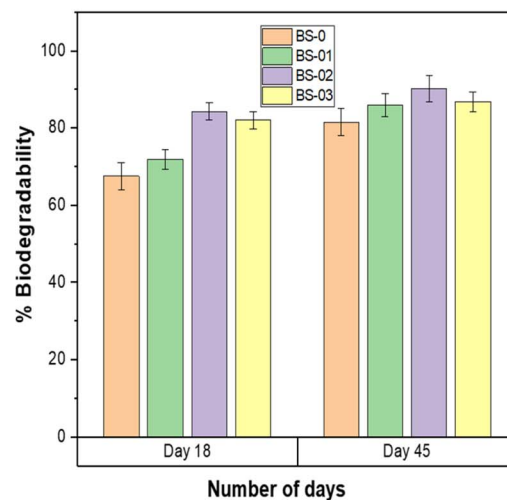
Table 4 Antioxidant activities of all samples

Sample code	DPPH assay		
	Percent inhibition of the DPPH free radical		
	0.5 mg mL <sup>-1</sup>	1 mg mL <sup>-1</sup>	IC <sub>50</sub> mg mL <sup>-1</sup>
BS-0	23.20 ± 1.3	47.0 ± 0.51	1.1
BS-01	33.1 ± 0.4	58.23 ± 1.3	0.7
BS-02	48.8 ± 1.3	70.5 ± 0.57	0.5
BS-03	55.0 ± 2.0	78.8 ± 1.01	0.3
Positive control (ascorbic acid)	70.08 ± 1.3	87.14 ± 0.26	0.36



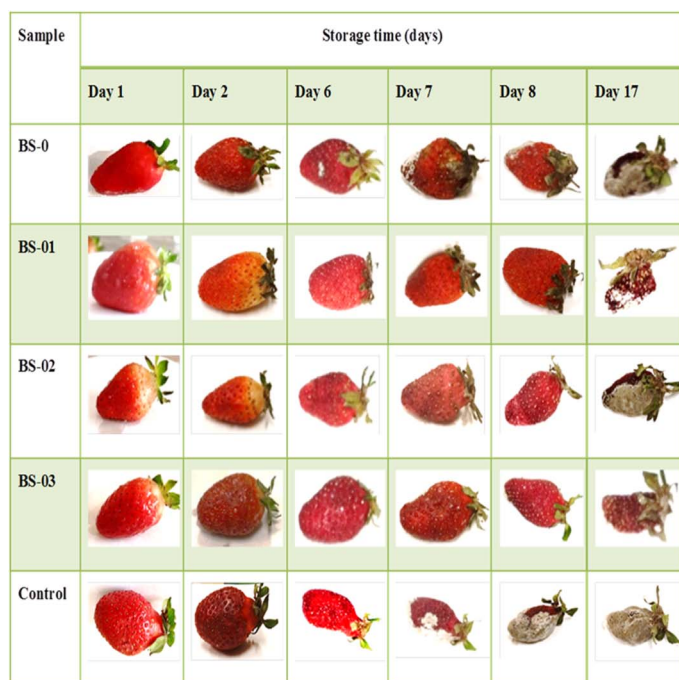


(A)

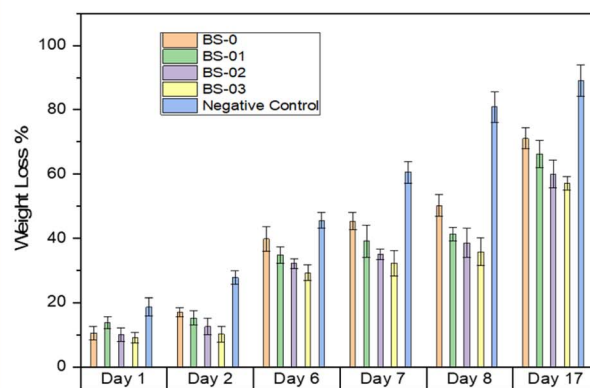


(B)

Fig. 12 (A) Images of composite films (a) BS-0, (b) BS-01, (c) BS-02, and (d) BS-03 before experimentation; (e) BS-0, (f) BS-01, (g) BS-02, and (h) BS-03 after day 18; (i) BS-0, (j) BS-01, (k) BS-02, and (l) BS-03 after day 45; (B) % biodegradability at day 18 and day 45 of the prepared films.



(A)



(B)

Fig. 13 (A) Images representing application of coatings on strawberries and their deterioration with respect to the number of days; control represents uncoated strawberries. (B) Weight loss % of strawberries from day 1 to day 17.

a key source of many raw materials for cosmetics, herbal teas and rose oil.<sup>87</sup> The TPCs and TFCs of *Rosa rubiginosa* extract (RRE) are expressed in  $\mu\text{g}$  of gallic acid equivalent (GAE) and  $\mu\text{g}$  of quercetin equivalent (QE) per mg of extract, respectively. The TPCs of RRE were found to be  $86.74 \pm 0.91 \mu\text{g GAE per mg}$ .

These values are close to those described by Murathan *et al.*<sup>88</sup> and Fascella *et al.*<sup>89</sup> Literature studies have demonstrated that among phenolic compounds, *p*-coumaric acid and chlorogenic acid were present abundantly in RRE extract. It was observed that the phytochemical properties of various rose species are



greatly dependent upon their type of species. The RRE was found to be a promising source of natural antioxidants, which are useful in the pharmaceutical and food industries.<sup>90</sup> Similarly, TFCs of RRE were found to be  $26.73 \pm 0.68 \mu\text{g QE per mg}$ . These values were also in accordance with already reported values by Tabaszewska *et al.*<sup>91</sup> Quercetin and luteolin are key flavonoid aglycons in rose species. Quercetin and luteolin belong to the flavonol and flavone groups, respectively.<sup>92</sup>

### 3.16 Application on strawberries

Coatings offer an effective solution to extend the shelf life of fruits and vegetables. Strawberries, being delicate and water-rich, have a limited shelf life and are prone to spoilage after harvesting due to pathogen attacks. Unpackaged or uncoated foods also deteriorate due to water evaporation and cellular respiration. All the composite coating solutions of BS-0, BS-01, BS-02 and BS-03 were used for application on strawberries to evaluate their potential to protect and enhance the shelf life of strawberries. Uncoated strawberries were used as a negative control for comparison of results. The weight loss % was monitored after the 1st, 2nd, 6th, 7th, 8th and 17th day. Fig. 13 (A) and (B) represent the results in terms of images of strawberries and weight loss % over time (in days), respectively. The results indicated that coating solutions with higher RRE ratios exhibited better protection of strawberries and provided greater shelf life, as indicated by both images and weight loss % graphs. Similar results have also been discussed in the literature by Mukhtar *et al.*<sup>93</sup> The results showed that uncoated strawberries (control) started to deteriorate slowly after the 2nd day and experienced a 60% weight loss after the 7th day. For coated strawberries using BS-0, BS-01, BS-02, and BS-03 coating solutions, the weight loss percentages on day 6 were 39.82%, 34.87%, 32.12%, and 29.28%, respectively, compared to 45.55% for uncoated strawberries. Similarly, after the 7th day, the weight loss % was 45.35% for BS-0, 39.09% for BS-01, 35.05% for BS-02, 32.23% for BS-03 and 60.59% for the negative control. It can be inferred from Fig. 13(A) that the initial weight loss up to 6 days was mainly due to the loss of water content from strawberries, and then after 6 or 7 days, fungal attack began, which started to degrade the strawberries.

By day 17, weight loss % reached 71.09% for BS-0, 66.32% for BS-01, 60.07% for BS-02, 57.2% for BS-03 and 89.03% for the uncoated negative control. It was noted that all coating solutions preserved strawberries well and enhanced their shelf life up to 8 days without being deteriorated by fungal attack. After 8 days, the strawberries coated with BS-0, BS-01 and BS-02 started to deteriorate by fungal attack more rapidly as compared to those coated with BS-03 solution, which remained intact up to 10 days. Thus, it can be concluded that increasing the volume ratio of RRE in CS/PVA/gelatin-based coating solutions has enhanced the shelf life of strawberries up to 10 days. The BS-03 coating solution demonstrated the best performance in reducing % weight loss, suggesting its highest potential for preserving delicate food items. The results of fabricated coatings on strawberries were also compared with literature studies, and the results are presented in Table S1 in the SI. The literature studies reported that the strawberries were stored for 5 days at room temperature and

for 15 days at 4 °C, but our fabricated coatings protected strawberries for 10 days at room temperature.

### 3.17 Sensory evaluation

The results of sensory evaluation for each formulation coded as BS-0, BS-01, BS-02 and BS-03 and a control (without any coating) are presented in Tables S2–S6. The results showed that strawberries coated with the BS-03 formulation showed the most favourable and better results in terms of taste, smell, color, juiciness, firmness and acceptability in general as compared to BS-0, BS-01 and BS-02 formulations.

This might be due to the presence of the highest amount of RRE in this formulation, which provided enhanced antioxidant and antibacterial properties to this formulation. The BS-0 formulation exhibited results of parameters such as taste, smell, color, juiciness, firmness and general acceptability mostly in “neither good nor bad” and “like somewhat” categories. Similarly, BS-01 showed most of the studied parameters in the “like somewhat” category. The BS-02 coating exhibited parameters in “like somewhat” and “moderate” categories. The BS-03 coating showed the most attractive and convincing results of studied parameters in the “similar to moderate” and “greatly admire” categories. The control strawberries without any coating were subjected to the highest degradation and changes, thus their study parameters mostly fall under “mildly disliked” and “mildly unfavourable” categories.

## 4. Conclusion

This study demonstrated that CS/PVA/gelatin composite coatings enriched with RRE enhanced the preservation of strawberries. Increasing the RRE volume ratio in CS/PVA/gelatin coatings (from BS-01 to BS-03) thickened the films and improved their barrier performance, while % moisture content, water solubility water absorption, and oxygen permeability were decreased. Antimicrobial tests showed that coatings containing a higher volume of RRE, particularly BS-02 and BS-03, exhibited stronger activities against *S. aureus*, *B. subtilis*, and *E. coli* than the RRE free coating (BS-0). Antioxidant capacity also increased with enhancing RRE ratio, with BS-03 reaching  $78.8 \pm 1.01\%$  DPPH inhibition ( $\text{IC}_{50} = 0.3 \text{ mg mL}^{-1}$ ). Soil burial trials confirmed that all films were biodegradable; the highest 45-day weight loss was observed for BS-02 (91.29%), followed by BS-03 (86.79%). Although the incorporation of RRE reduced ductility and increased stiffness, the mechanical properties of the BS-03 film would be more suitable for handling and packaging applications. When applied to strawberries, all coatings helped reduce weight loss compared to the uncoated control and prolonged their shelf life. Among them, BS-03 was the most effective, preventing visible spoilage for up to 10 days and achieving the highest sensory scores. Overall, the BS-03 formulation emerges as a promising bio-based coating for the short-term extension of strawberries shelf life. Future research should focus on optimizing composition through response surface methodology, conducting anti-fungal tests, evaluating performance during refrigerated storage, and examining component migration for applications involving direct contact with food.



## Author contributions

B. S.: conducted experiments, investigations, data analysis and writing – original draft. M. Z.: conceptualization, writing – original draft, reviewing and editing. A. Y.: performed antibacterial assessment. F. A.: reviewing. S. S.: conceptualization, supervision, editing and reviewing. A. U.: conceptualization, supervision, editing and reviewing. All authors have read and agreed to the published version of the manuscript.

## Conflicts of interest

There are no conflicts to declare.

## Data availability

The data supporting this article have been included as part of the Supplementary Information (SI). Supplementary information: the tables have been cited in the manuscript. Table S1 cited in Section 3.16 and Tables S2–S6 cited in Section 3.17. While the Fig. S3 is cited in the Section 2.2.1. See DOI: <https://doi.org/10.1039/d5fb00934k>.

## References

- 1 L. Kalra, R. Anushree and A. W. Sultani, *Indian J. Ecol.*, 2024, **51**, 697–706.
- 2 FAO, *The State of Food and Agriculture 2019: Moving Forward on Food Loss and Waste Reduction*, UN, 2019.
- 3 L. Brennan, S. Langley, K. Verghese, S. Lockrey, M. Ryder, C. Francis, N. T. Phan-Le and A. Hill, *J. Clean. Prod.*, 2021, **281**, 125276.
- 4 S. Wardejn, S. Waclawek and G. Dudek, *Int. J. Mol. Sci.*, 2024, **25**, 12580.
- 5 S. Sumnu and L. Bayindirli, *J. Sci. Food Agric.*, 1995, **67**, 537–540.
- 6 L. Pavoni, D. R. Perinelli, G. Bonacucina, M. Cespi and G. F. Palmieri, *Nanomaterials*, 2020, **10**, 135.
- 7 F. Salehi, *Int. J. Fruit Sci.*, 2020, **20**, S570–S589.
- 8 A. F. Pires, O. Díaz, A. Cobos and C. D. Pereira, *Foods*, 2024, **13**, 2638.
- 9 M. Mujtaba, R. E. Morsi, G. Kerch, M. Z. Elsabee, M. Kaya, J. Labidi and K. M. Khawar, *Int. J. Biol. Macromol.*, 2019, **121**, 889–904.
- 10 F. Mohanty and S. Swain, in *Nanotechnology Applications in Food*, Elsevier, 2017, pp. 363–379.
- 11 E. Ojogbo, E. O. Ogunsona and T. H. Mekonnen, *Mater. Today Sustain.*, 2020, **7**, 100028.
- 12 Z. Wu, J. Wu, T. Peng, Y. Li, D. Lin, B. Xing, C. Li, Y. Yang, L. Yang and L. Zhang, *Polymers*, 2017, **9**, 102.
- 13 N. Ruocco, S. Costantini, S. Guariniello and M. Costantini, *Molecules*, 2016, **21**, 551.
- 14 M. Friedman and V. K. Juneja, *J. Food Prot.*, 2010, **73**, 1737–1761.
- 15 M. Kong, X. G. Chen, K. Xing and H. J. Park, *Int. J. Food Microbiol.*, 2010, **144**, 51–63.
- 16 L. A. van den Broek, R. J. Knoop, F. H. Kappen and C. G. Boeriu, *Carbohydr. Polym.*, 2015, **116**, 237–242.
- 17 M. A. Del Nobile, N. Di Benedetto, N. Suriano, A. Conte, M. R. Corbo and M. Sinigaglia, *Food Microbiol.*, 2009, **26**, 587–591.
- 18 A. Verlee, S. Mincke and C. V. Stevens, *Carbohydr. Polym.*, 2017, **164**, 268–283.
- 19 M. Hosseinejad and S. M. Jafari, *Int. J. Biol. Macromol.*, 2016, **85**, 467–475.
- 20 D. C. Vodnar, O. L. Pop, F. V. Dulf and C. Socaciu, *Not. Bot. Horti Agrobot. Cluj-Napoca*, 2015, **43**, 302–312.
- 21 N. A. Al-Tayyar, A. M. Youssef and R. Al-Hindi, *Food Chem.*, 2020, **310**, 125915.
- 22 M. Z. Elsabee and E. S. Abdou, *Mater. Sci. Eng., C*, 2013, **33**, 1819–1841.
- 23 F. Jahan, R. Mathad and S. Farheen, *Mater. Today: Proc.*, 2016, **3**, 3689–3696.
- 24 J. Khouri, A. Penlidis and C. Moresoli, *Processes*, 2019, **7**, 157.
- 25 H. Haghghi, F. Licciardello, P. Fava, H. W. Siesler and A. Pulvirenti, *Food Packaging and Shelf Life*, 2020, **26**, 100551.
- 26 T. Yeamsuksawat and J. Liang, *Food Packag. Shelf Life*, 2019, **22**, 100415.
- 27 E. Aguila-Almanza, R. Salgado-Delgado, Z. Vargas-Galarza, E. García-Hernández and H. Hernández-Cocoletzi, *J. Chem.*, 2019, **2019**, 1–8.
- 28 W. M. Argüelles-Monal, J. Lizardi-Mendoza, D. Fernández-Quiroz, M. T. Recillas-Mota and M. Montiel-Herrera, *Polymers*, 2018, **10**, 342.
- 29 X.-Y. Wang, C.-S. Wang and M.-C. Heuzey, *Int. J. Polym. Mater. Polym. Biomater.*, 2016, **65**, 96–104.
- 30 J. Wang, L. Wang, H. Yu, Y. Chen, Q. Chen, W. Zhou, H. Zhang and X. Chen, *Int. J. Biol. Macromol.*, 2016, **88**, 333–344.
- 31 K. Khwaldia, A. H. Basta, H. Aloui and H. El-Saied, *Carbohydr. Polym.*, 2014, **99**, 508–516.
- 32 E. Abdelrazek, I. Elashmawi and S. Labeeb, *Phys. B*, 2010, **405**, 2021–2027.
- 33 M. Shahbazi, G. Rajabzadeh and S. J. Ahmadi, *Carbohydr. Polym.*, 2017, **157**, 226–235.
- 34 A. Muxika, A. Etxabide, J. Uranga, P. Guerrero and K. De La Caba, *Int. J. Biol. Macromol.*, 2017, **105**, 1358–1368.
- 35 H. Wang, J. Qian and F. Ding, *J. Agric. Food Chem.*, 2018, **66**, 395–413.
- 36 E. A. Kamoun, E.-R. S. Kenawy and X. Chen, *J. Adv. Res.*, 2017, **8**, 217–233.
- 37 S. Mohanapriya, *Polyvinyl Alcohol-Based Biocomposites and Bionanocomposites*, 2023, pp. 59–79.
- 38 J. Zanela, A. P. Bilck, M. Casagrande, M. V. E. Grossmann and F. Yamashita, *Polímeros*, 2018, **28**, 256–265.
- 39 D. Gu, Y. Yang, M. Bakri, Q. Chen, X. Xin and H. A. Aisa, *Phytochem. Anal.*, 2013, **24**, 661–670.
- 40 B. Hamed, A. G. Pirbalouti and F. Rajabzadeh, *Ind. Crops Prod.*, 2022, **187**, 115470.
- 41 H.-J. Choi, S.-W. Choi, N. Lee and H.-J. Chang, *Foods*, 2022, **11**, 3963.
- 42 S. Islam, V. Jaiswal, B. Butola and A. Majumdar, *Int. J. Biol. Macromol.*, 2023, **252**, 126457.



- 43 Y. Wang, Y. Yu, C. Shi, Y. Ren, J. Han and R. Wu, *Int. J. Biol. Macromol.*, 2025, **308**, 142299.
- 44 J. F. Rubilar, R. M. Cruz, H. D. Silva, A. A. Vicente, I. Khmelinskii and M. C. Vieira, *J. Food Eng.*, 2013, **115**, 466–474.
- 45 V. G. Bhat, S. S. Narasagoudr, S. P. Masti, R. B. Chougale, A. B. Vantamuri and D. Kasai, *Int. J. Biol. Macromol.*, 2022, **200**, 50–60.
- 46 M. Mujahid, M. Zubair, A. Yaqoob, S. Shahzad and A. Ullah, *Bioengineering*, 2025, **12**, 439.
- 47 A. Hassan, M. B. K. Niazi, A. Hussain, S. Farrukh and T. Ahmad, *J. Polym. Environ.*, 2018, **26**, 235–243.
- 48 S. Shahzad, S. Ahmed, A. Yaqoob, S. Saleem, S. Shaheen, K. Mammadova, A. K. Qureshi, M. Arshad, A. Saeed and D. H. M. Alkhalifah, *Chem. Pap.*, 2025, 1–16.
- 49 S. Vasi, G. Ceccio, A. Cannavò, P. Pleskunov and J. Vacík, *Sustainability*, 2022, **14**, 5863.
- 50 D. Yun and J. Liu, *Foods*, 2024, **13**, 1174.
- 51 L. W. Winkler, *Ber. Dtsch. Chem. Ges.*, 1888, **21**, 2843–2854.
- 52 H. Bauer, F. Paronetto, W. A. Burns and A. Einheber, *J. Exp. Med.*, 1966, **123**, 1013–1024.
- 53 M. Abbas, M. Arshad, M. Rafique, A. Altalhi, D. Saleh, M. Ayub, S. Sharif, M. Riaz, S. Alshawwa and N. Masood, *Arab. J. Chem.*, 2022, **15**, 103766.
- 54 T. Wang, X. Zhai, X. Huang, Z. Li, X. Zhang, X. Zou and J. Shi, *Food Packag. Shelf Life*, 2023, **39**, 101133.
- 55 M. Nowacka, K. Rybak, A. Wiktor, A. Mika, P. Boruszewski, J. Woch, K. Przybysz and D. Witrowa-Rajchert, *Food Control*, 2018, **93**, 183–190.
- 56 F. Nugroho, N. Nizardo and E. Saepudin, *AIP Conf. Proc.*, 2020, **2242**, 040040.
- 57 D. Yun, Y. Qin, J. Zhang, M. Zhang, C. Qian and J. Liu, *Int. J. Biol. Macromol.*, 2021, **189**, 900–909.
- 58 M. Zubair, S. Hussain, A. Hussain, M. E. Akram, S. Shahzad, Z. Rauf, M. Mujahid and A. Ullah, *Biomater. Sci.*, 2025, **13**, 130–160.
- 59 N. K. Howell, G. Arteaga, S. Nakai and E. C. Li-Chan, *J. Agric. Food Chem.*, 1999, **47**, 924–933.
- 60 M. Cantor, E. Buta, I. Conțiu, R. Ștefan, I. Crișan and T. Buru, *Emir. J. Food Agric.*, 2021, **33**, 899–908.
- 61 R. Różyło, R. Amarowicz, M. A. Janiak, M. Domin, I. Różyło, K. Rząd, A. Matwijczuk, R. Rusinek and M. Gancarz, *Molecules*, 2024, **29**, 4931.
- 62 D. Hu, X. Liu, Y. Qin, J. Yan, J. Li and Q. Yang, *Food Qual. Saf.*, 2022, **6**, fyac028.
- 63 G. Qiao, Z. Xiao, W. Ding and A. Rok, *Coatings*, 2019, **9**, 828.
- 64 D. Lin and Y. Zhao, *Compr. Rev. Food Sci. Food Saf.*, 2007, **6**, 60–75.
- 65 Y. Peng, Y. Wu and Y. Li, *Int. J. Biol. Macromol.*, 2013, **59**, 282–289.
- 66 U. Siripatrawan and B. R. Harte, *Food Hydrocoll.*, 2010, **24**, 770–775.
- 67 X. Wang, H. Yong, L. Gao, L. Li, M. Jin and J. Liu, *Food Hydrocoll.*, 2019, **89**, 56–66.
- 68 F. Bigi, H. Haghighi, H. W. Siesler, F. Licciardello and A. Pulvirenti, *Food Hydrocolloids*, 2021, **120**, 106979.
- 69 H.-S. Han and K. B. Song, *Food Hydrocolloids*, 2021, **112**, 106372.
- 70 T. A. Dinh, Y. N. Le, N. Q. Pham, P. Ton-That, T. Van-Xuan, T. G.-T. Ho, T. Nguyen and H. H. K. Phuong, *Prog. Org. Coat.*, 2023, **183**, 107772.
- 71 Annu, A. Ali and S. Ahmed, *Heliyon*, 2021, **7**(3), e06550.
- 72 L. Wang, Y. Dong, H. Men, J. Tong and J. Zhou, *Food Hydrocoll.*, 2013, **32**, 35–41.
- 73 S. B. Gheleju, M. Esmaili and H. Almasi, *Int. J. Biol. Macromol.*, 2016, **86**, 613–621.
- 74 J. Hafsa, M. ali Smach, M. R. B. Khedher, B. Charfeddine, K. Limem, H. Majdoub and S. Rouatbi, *LWT-Food Sci. Technol.*, 2016, **68**, 356–364.
- 75 S. Yadav, G. Mehrotra, P. Bhartiya, A. Singh and P. Dutta, *Carbohydr. Polym.*, 2020, **227**, 115348.
- 76 C. Pagella, G. Spigno and D. M. De Faveri, *Food Bioprod. Process.*, 2002, **80**, 193–198.
- 77 B. Singh, J. Singh, V. Sharma, P. Sharma and R. Kumar, *Hybrid Adv.*, 2023, **4**, 100096.
- 78 N. Nowak, W. Grzebieniarz, A. Cholewa-Wójcik, L. Juszcak, A. Konieczna-Molenda, E. Dryzek, M. Sarnek, M. Szuwarzyński, T. Mazur and E. Jamróz, *Food Bioprocess Technol.*, 2024, **17**, 1201–1214.
- 79 L. K. Winkelströter, E. Bezirtzoglou and F. L. Tulini, *Front. Microbiol.*, 2022, **13**, 1–3.
- 80 D. Altiok, E. Altiok and F. Tihminlioglu, *J. Mater. Sci.: Mater. Med.*, 2010, **21**, 2227–2236.
- 81 Y. Xing, Q. Xu, X. Li, C. Chen, L. Ma, S. Li, Z. Che and H. Lin, *Int. J. Polym. Sci.*, 2016, **2016**, 4851730.
- 82 D. Xu, T. Chen and Y. Liu, *Polym. Bull.*, 2021, **78**, 3607–3624.
- 83 M. Moghadam, M. Salami, M. Mohammadian, M. Khodadadi and Z. Emam-Djomeh, *Food Hydrocolloids*, 2020, **104**, 105735.
- 84 A. Riaz, C. Lagnika, H. Luo, Z. Dai, M. Nie, M. M. Hashim, C. Liu, J. Song and D. Li, *Int. J. Biol. Macromol.*, 2020, **150**, 595–604.
- 85 T. Gasti, S. Dixit, S. P. Sataraddi, V. D. Hiremani, S. P. Masti, R. B. Chougale and R. B. Malabadi, *J. Polym. Environ.*, 2020, **28**, 2918–2930.
- 86 J. B. Harborne, *Phytochemistry*, 1983, **22**, 1683–1684.
- 87 S. Kayahan, F. Gülbağ, Y. Kaya and H. Altunkanat, *Hortic. Stud.*, 2024, **41**, 74–81.
- 88 Z. T. Murathan, M. Zarifkhosroshahi, E. Kafkas and E. Sevindik, *Ital. J. Food Sci.*, 2016, **28**, 314–325.
- 89 G. Fascella, F. D'Angiolillo, M. M. Mammano, M. Amenta, F. V. Romeo, P. Rapisarda and G. Ballistreri, *Food Chem.*, 2019, **289**, 56–64.
- 90 S. Shameh, B. Hosseini, A. Alirezalu and R. Maleki, *J. AOAC Int.*, 2018, **101**, 1788–1793.
- 91 M. Tabaszewska and D. Najgebauer-Lejko, *NFS J.*, 2020, **21**, 50–56.
- 92 A. Y. Aldhebiani and W. A. Yaslam, *Pak. J. Bot.*, 2023, **55**, 995–999.
- 93 N. Mukhtar, N. A. Marzuki, N. M. Zain, L. Naher, N. M. Hairin and N. M. Arsab, *IOP Conf. Ser.: Earth Environ. Sci.*, 2024, **1397**, 1–9.

